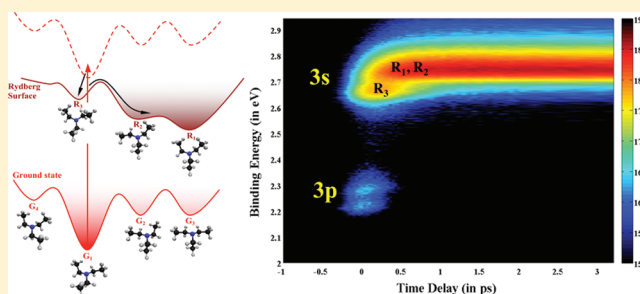


# Structural Dynamics in Floppy Systems: Ultrafast Conformer Motions in Rydberg-Excited Triethylamine

Sanghamitra Deb, Brian A. Bayes,<sup>†</sup> Michael P. Minitti, and Peter M. Weber\*

Department of Chemistry, Brown University, Providence, Rhode Island 02912, United States

**ABSTRACT:** Rotations about its three carbon–nitrogen bonds give triethylamine a complex, 3-dimensional potential energy landscape of conformeric structures. Electronic excitation to Rydberg states prepares the molecule in a high-energy, nonequilibrium distribution of such conformers, initiating ultrafast transitions between them. Time-resolved Rydberg electron binding energy spectra, observed using photoionization-photoelectron spectroscopy with ultrashort laser pulses, reveal these time-evolving structures. The time-dependent structural fingerprint spectra are assigned with the aid of a computational analysis of the potential energy landscape. Upon 209 nm electronic excitation to the 3p Rydberg state, triethylamine decays to 3s with a 200 fs time constant. The initially prepared conformer reacts to a mixture of structures with a time constant of 232 fs and settles into a final geometry distribution on a further subpicosecond time scale. The binding energy of the Rydberg electron is found to be an important determinant of the conformeric energy landscape.



## INTRODUCTION

Conformational dynamics is at the heart of many of today's most prominent scientific questions, from protein folding<sup>1,2</sup> and enzyme function<sup>3</sup> to molecular motors.<sup>4</sup> To explore such molecular motions in depth, it is important to understand and characterize conformational changes in small molecules with the minimum necessary complexity. Triethylamine (TEA) has three “backbone” rotations about C–N bonds<sup>5</sup> that provide structural flexibility, creating a richly structured potential energy landscape. The steric interactions between the three ethyl chains cause strong coupling, making for complex conformeric motions. We use Rydberg fingerprint spectroscopy<sup>6–8</sup> measurements, supplemented by an analysis using density functional theory, to derive a detailed understanding of how highly energized TEA molecules explore the energy landscape as they approach conformational equilibrium in the presence of strong coupling.

Time-resolved Rydberg fingerprint spectroscopy (TR-RFS) is a versatile tool<sup>9,10</sup> that takes advantage of the unique properties of Rydberg states. Molecular Rydberg states are excited electronic states with wave functions that resemble the Rydberg orbitals of the hydrogen atom ( $n \geq 3$ ). Even in polyatomic molecules, Rydberg orbitals are often diffuse enough to extend across the entire molecule, and yet their energies are remarkably sensitive to subtle changes in molecular structure<sup>6–8,11</sup> including conformation.<sup>12,13</sup> Additionally, since the electronic transition spectra from the Rydberg state to the ion are not broadened by molecular vibrations,<sup>14,15</sup> temperature effects do not distort or otherwise obscure these binding energy spectra. As a result, RFS can be used on hot molecules: even flexible molecules that have sufficient energy to transition between conformers can be observed at high resolution.<sup>16,17</sup> Finally, the RFS technology can be combined

with the well-established pump–probe methodology to determine the time-dependent changes in molecular geometry, with a time resolution that is determined only by the duration and jitter of the laser pulses.<sup>18</sup> The combination of high sensitivity, broad spatial sampling, and high time resolution makes TR-RFS an ideal sensor for investigating phenomena involving structural dynamics.

To study the conformational dynamics of TEA, we optically excite the system from the ground electronic state to the 3p Rydberg state (Figure 1). This excitation lifts a nonbonding electron from the amine group to the delocalized Rydberg orbit.<sup>19</sup> The molecule responds by changing its structure along the amine's umbrella coordinate from a pyramidal to an approximately planar geometry. The transition to the Rydberg state leads, by the Franck–Condon principle, to the side of the well of the umbrella motion coordinate, depositing about 0.7 eV of energy into vibrational motions. The molecule acquires additional vibrational energy when it crosses to 3s in a process that we observe to occur on a subpicosecond time scale. The energy so inserted into the vibrational manifold is sufficient to allow for transformations between conformeric structures that are associated with the rotation of ethyl groups about the C–N bond axes. To probe the conformeric structural dynamics, we ionize with a time delayed probe pulse. This lifts the molecules to the ion surface, which features a conformeric energy landscape that is similar to, but not identical with, the Rydberg surface. The

Received: November 15, 2010

Revised: January 10, 2011

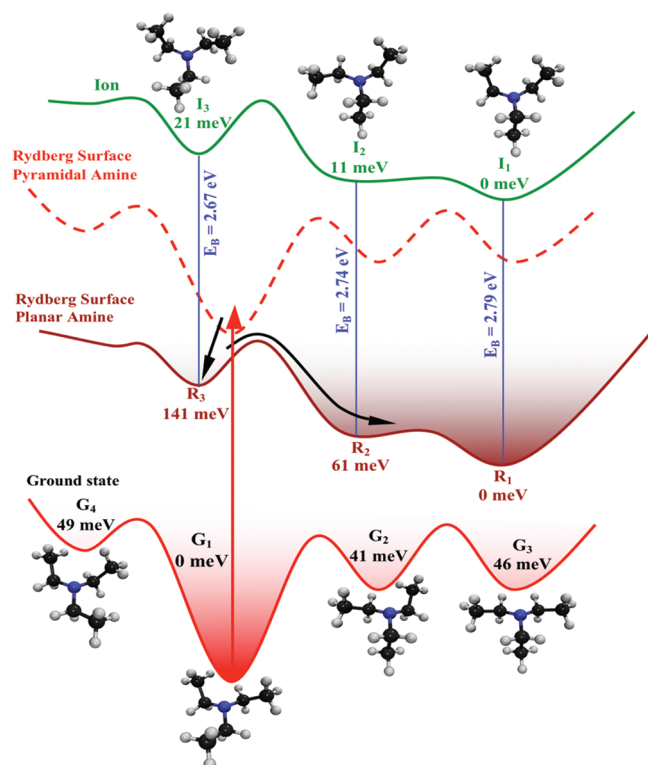


**Figure 1.** Schematic illustration of the potential energy landscapes of the conformeric structures of triethylamine, where the vertical scale represents energy. The ground-state landscape is characterized by four minima, labeled  $G_1$  through  $G_4$ , with energies derived from the computations as discussed in the text. The ion and Rydberg states have three conformeric minima. In the experiment, the ground-state surface and population are projected onto the Rydberg state (dashed curve, pyramidal amine). The initial excitation is to  $3p$ , followed by rapid decay to  $3s$ . Since the conformeric energy landscapes are not dramatically affected by the electronic transition, the  $3p \rightarrow 3s$  decay is not shown in the illustration of the conformeric coordinate. The initially projected (pyramidal) conformeric landscape rapidly adjusts to its new shape (solid Rydberg line, planar amine), inducing the conformeric dynamics that is probed by recording the time-dependent electron binding energies  $E_B$ .

ejected electrons are observed and their energy recorded as a function of delay time between pump and probe pulses.

Conformeric dynamics arises because of both the greatly altered potential energy landscape associated with the planarization of the amine group and the rapidly increased internal energy available to sample this landscape upon optical excitation. When TEA explores this energy landscape, the ethyl groups rotate about the C–N single bonds and the methyl groups rotate about the C–C bonds. In most molecular geometries, the methyl rotations have a small barrier,<sup>20,21</sup> so that this motion is probably quickly thermalized. Each of the three ethyl groups, however, moves in a sterically confined space defined by the other ethyl groups. Rotation of one ethyl group requires adjustments in the position of the others. These coupled and mutually restrictive rotations of the ethyl groups slow down the structural dynamics such that it can be observed on a subpicosecond to picosecond time scale using optical pump–probe methods.

The present work builds on a previous study of the conformational dynamics in dimethyl-2-butanamine (DM2BA).<sup>13</sup> In that system, only two conformers are involved in the structural

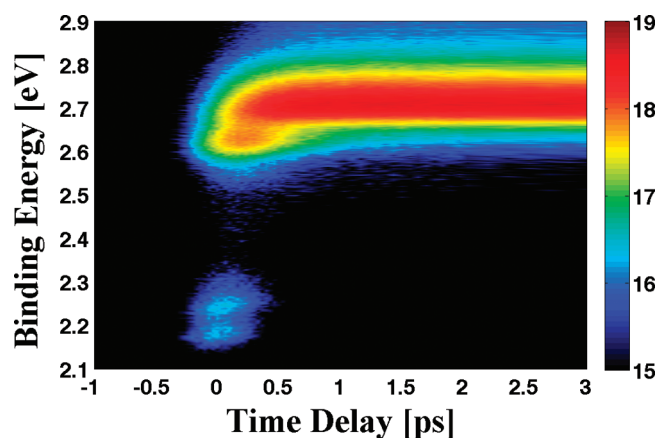


**Figure 2.** Time-dependent Rydberg electron binding energy spectrum of TEA upon excitation with one photon at 209 nm and ionization at 418 nm. The color represents the intensity on a logarithmic scale; the color bar gives the natural logarithm of the intensities in arbitrary units.

dynamics, making for a much simpler conformational energy landscape. Moreover, the rotations were not as constrained as in TEA. But, because the barriers between conformers are higher, the time scale for the interconversion of conformers was longer, on the order of tens of picoseconds.

## EXPERIMENT

Details of the photoelectron-mass spectroscopy apparatus and the femtosecond laser system have been described previously.<sup>11,16,22</sup> For the time-resolved experiments described here we use a regenerative amplifier operating at a 5 kHz repetition rate, which produces pulses in the wavelength range 770–840 nm with  $\sim 70$  fs duration. The laser output is upconverted using BBO crystals, giving wavelengths of 418 and 209 nm for the second and fourth harmonics, respectively. The 209 and 418 nm laser pulses, focused into the molecular beam by a 200 mm lens to intensities of  $7 \times 10^{10}$  and  $1 \times 10^{10}$  W/cm<sup>2</sup>, respectively, were used for excitation to  $3p$  and for the ionization step. The time zero of the laser pulse overlap was determined by monitoring the cross-correlation time between the fourth harmonic excitation and second harmonic ionization pulses using the molecular response function of 1,4-dimethylpiperazine.

The molecular beam is generated by expanding TEA vapor, seeded at  $-30$  °C in helium as a carrier gas at 2 bar pressure, through a nozzle orifice with a 100  $\mu$ m diameter. The molecular beam is sampled by a 150  $\mu$ m skimmer and is oriented normally to the laser beam propagation axis. Anhydrous TEA was purchased from Sigma-Aldrich and used without further purification.

## RESULTS AND DISCUSSION

**Structural Dynamics Overview.** The time-resolved Rydberg fingerprint spectrum of TEA resulting from excitation at 209 nm is presented in Figure 2. Data were collected for delay times up to 100 ps, but only the time delay range from  $-1$  to  $+3$  ps is shown because that region exhibits interesting dynamics. The spectrum features two groups of clearly distinct peaks. On the basis of a significant body of previous work on related amine molecules,<sup>17,18,23,24</sup> we assign the very short-lived Rydberg peaks at 2.22 and 2.28 eV to  $3p$  states, and the peaks at 2.67 and 2.74 eV to  $3s$  states.

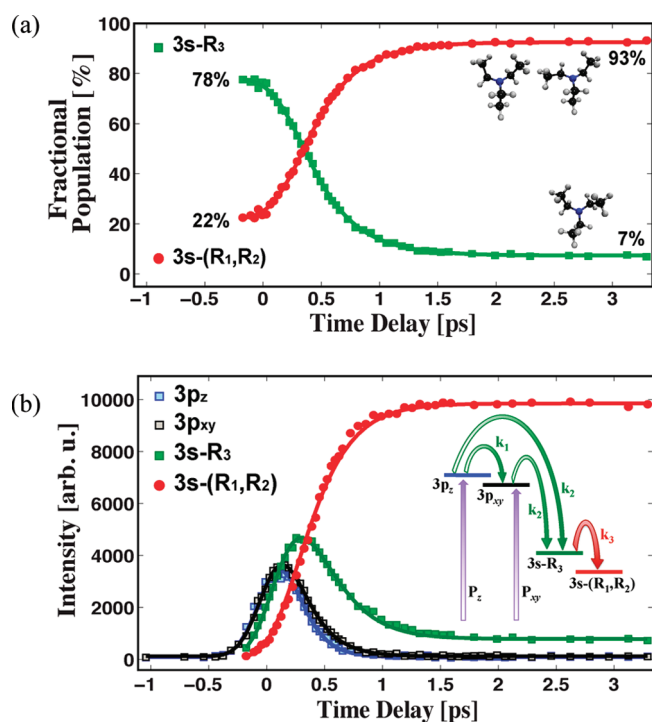


**Figure 3.** (a) Time-dependence of the fractional populations of conformers R<sub>3</sub> and the combined (R<sub>1</sub>,R<sub>2</sub>) conformers. The experimental data (symbols) were fitted to a theoretical model assuming a first order reaction between the conformers and a convolution with an instrument function. (b) The time-dependent signals of the different features (3p and 3s peak components) of the contour spectrum, Figure 2. The symbols are experimental data and the solid lines are fits using the kinetics scheme of panel b. The kinetics scheme (inset of Figure 3b) shows the electronic and conformeric decay pathways in the Rydberg states of TEA. P<sub>z</sub> and P<sub>xy</sub> represent the relative excitation probabilities in one-photon excitation to the corresponding 3p Rydberg states from the electronic ground state. The lower 3p<sub>xy</sub> states decay directly to 3s with a rate of k<sub>2</sub>; the higher 3p<sub>z</sub> states decay both into 3p<sub>xy</sub> and 3s, with rates k<sub>1</sub> and k<sub>2</sub>, respectively. The conformeric transition of R<sub>3</sub> to (R<sub>1</sub>,R<sub>2</sub>) in the 3s Rydberg state proceeds with a rate k<sub>3</sub>. The best fits, solid lines, were obtained with the parameters listed in Table 1.

Importantly, any Rydberg series of a molecule with a well-defined structure has only a single 3s state. In previous studies this led us to assign splittings in 3s Rydberg states of flexible molecules to conformationally distinct structures.<sup>13</sup> In TEA, the transient features of the 3s signal reveal that one well-defined conformeric structure exists only for a fraction of a picosecond. For 3p levels, the assignment is less obvious because in low symmetry molecules the 3p states may split either due to conformeric structures or due to the three angular momentum projections of the p-orbital. The contour plot, Figure 2, shows that the 3p states, whether due to the different angular momentum sublevels or due to conformers, quickly decay to 3s, and that once in 3s, there is a transformation from a conformer with low binding energy to another one with higher binding energy.

The time-resolved mass-spectrum (not shown) reveals only parent ions at both the initial and long delay times, with almost no fragmentation.

**Kinetic Model of Electronic Relaxation and Conformer Dynamics.** Because the conformer dynamics is independent of

**Table 1. Time Constants Obtained in a Global Fit of All Time-Dependent Data, Together with Uncertainties (3σ)**

parameter	fit parameters (3σ)
electronic transition 3p → 3s	$\tau_2 = 1/k_2 = 200$ fs (27 fs)
electronic transition 3p <sub>z</sub> → 3p <sub>xy</sub>	$\tau_1 = 1/k_1 = 1.1$ ps (150 fs)
conformational dynamics R <sub>3</sub> → R <sub>1</sub> ,R <sub>2</sub>	$\tau_3 = 1/k_3 = 232$ fs (30 fs)
excitation probability	P <sub>z</sub> /P <sub>xy</sub> = 1.21

the electronic relaxation, a careful analysis of the ultrafast transients allows us to identify the source of the splitting of the 3p peak. To do so, we fitted the overlapping 3s peaks using asymmetric peak shapes, yielding time-dependent fractional populations, Figure 3a. The time-dependent transients, Figure 3b, are obtained by multiplying the overall time-dependent 3s intensity by the fractional populations.

A model that assumes that the 3p splitting arises from different conformeric forms did not give acceptable fits. The model that postulates that only one conformer is dominant in the ground state, and excited to two different 3p states by the 209 nm pulse, is consistent with the data, giving rise to the fits displayed as solid lines in Figure 3. As illustrated in the inset in Figure 3b, both of these 3p levels decay to 3s with a common time constant of k<sub>2</sub> = 1/200 fs, but there is also a slower transition between the 3p levels with a time constant of k<sub>1</sub> = 1/1.1 ps. The transition to 3s initially yields a distribution with 78% of the molecules in the high-energy conformer form with a binding energy of 2.67 eV (R<sub>3</sub> in Figure 1; see assignment below). The subsequent conformational dynamics within 3s, which leads to a distribution of conformers (R<sub>1</sub>,R<sub>2</sub>) with binding energies between 2.7 and 2.87 eV, is facile and fast, proceeding with a time constant of k<sub>3</sub> = 1/232 fs. The kinetic parameters of this fit are listed in Table 1.

The alternative interpretation of the 3p peaks as arising from two different conformers does not result in a self-consistent analysis. In particular, a model that assumes different conformers present in the ground state before excitation, and that interprets the split 3p peaks as due to conformeric forms, results in contradictory conformer distributions in 3s and 3p at certain time points. It is also inconsistent with the calculated oscillator strengths of the optical transitions.<sup>25</sup> We therefore conclude that only one conformer is initially present in the ground state, implying that TEA is effectively cooled in the molecular beam. A further argument supporting this conclusion is described later in the paper. We note that this observation is different from our previous experiment with DM2BA,<sup>13</sup> where conformers were found to be frozen in their room temperature distribution. This discrepancy between the two isomeric systems is quite intriguing and further discussed below.

**Assignment of Conformer Spectra.** Despite the unique capability of time-resolved RFS to unravel structural dynamics, there exists no general method for assigning spectral features to particular molecular geometries. The calculation of structure-dependent electron binding energies, i.e., the difference between the energies of the ion and the Rydberg state for a given molecular structure, remains a formidable computational challenge, largely because the diffuse Rydberg states are difficult to calculate. We therefore base the assignment on the computation of the energy landscapes of the molecular ground state and the ion state, and on the observed time-dependent binding energy spectra.

The assignment procedure is as follows. By comparing the geometries of conformers in the ground state and in the ion state,



we can identify which excited-state conformer(s) are initially generated. From the calculated ion-state surface and the measured binding energy spectrum we obtain the energies of the conformers in the Rydberg state. Given that we can infer the internal energy of the molecules in the Rydberg states from the energetics and the laser photon energies, the energies of the Rydberg-state conformers also yield the distribution after equilibrium is reached. Finally, matching that distribution with the observed time-dependent spectrum allows us to assign the binding energy peaks to the calculated molecular geometries. This procedure gives a unique assignment. Additionally, the structure-dependent relative energies of Rydberg states determine their relative populations, which are reflected as intensities in the ionization spectra. The measured binding energies are therefore related to the respective intensities of the observed peaks, providing a unique self-consistency check of the assignment.

In TEA, the four lowest-energy ground-state conformers are determined by a DFT–B3LYP/6-311++G(d,p) calculation using Spartan'08 and verified by calculations with Gaussian'03.<sup>26</sup> They are shown in Figure 1 and labeled  $G_1$  through  $G_4$  in order of ascending energy, with minimum energies of 0, 41, 46, and 49 meV. We also found that the energy barriers between these conformers are small compared to those in DM2BA,<sup>13</sup> which again supports our interpretation that only one TEA conformer is present in the molecular beam.

The energy landscape on which the conformeric dynamics takes place is the Rydberg-state surface, which differs significantly from the ground-state conformer landscape. Upon excitation, the geometry of TEA's amine core changes from pyramidal to approximately planar, affecting the steric interactions between ethyl branches. In the ion state the amine core is also planar, and its potential energy surface is quite similar to that of the Rydberg state, although the relative energies may vary. There are three preferred ion-state conformers, with structures as depicted in Figure 1, determined by a DFT–B3LYP/6-311++G(d,p) calculation. The energies of the minima on the ion landscape, are 0, 11, and 21 meV for structures  $I_1$ ,  $I_2$ , and  $I_3$ , respectively.

The absorption of a photon projects, at time zero, the ground state's pyramidal amine structure onto the Rydberg state (dashed potential energy curve in Figure 1). Once there, the planarization of the nitrogen core causes the conformeric energy landscape to rapidly evolve. To determine onto which of the excited-state conformations each ground-state conformer is projected (at time zero), direct energy-minimization calculations were performed, beginning with TEA cations bent into the preferred ground-state pyramidal form and conformations. Here we assume that the conformeric structures in the Rydberg state,  $R_1$ ,  $R_2$ , and  $R_3$ , are similar to those of the ion state,  $I_1$ ,  $I_2$ , and  $I_3$ . We found that conformers  $G_1$  and  $G_4$  adopt the  $R_3$  excited-state conformer structure, while conformers  $G_2$  and  $G_3$  map onto the  $R_2$  conformer. It is readily apparent that this mapping does not yield an equilibrium distribution of excited-state conformers: none of the molecules adopts the lowest-energy  $R_1$  conformer structure at time zero.

To reach the assignment of spectral peaks to conformeric structures, we conclude that at time zero, there is one dominant ground-state conformer with structure  $G_1$ , which is projected onto  $R_3$ . We consequently identify  $R_3$  as the high-energy conformer with binding energy 2.67 eV. The lower energy conformer with a binding energy between 2.7 and 2.87 eV must therefore belong to the conformeric structures of  $R_1$  and  $R_2$ . We

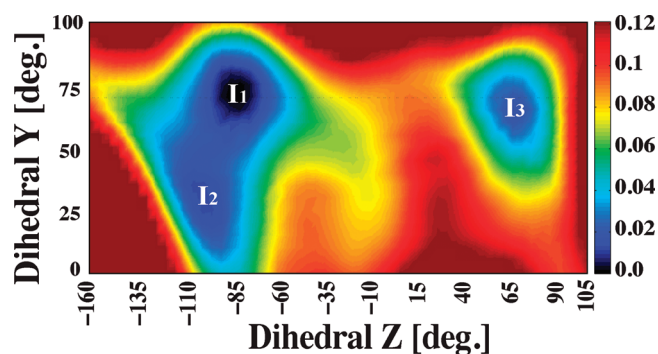


**Figure 4.** Potential energy surface along a selected plane through TEA's pseudo-three-dimensional ion-state conformer space. The horizontal and vertical axes represent two of three Me–C–N–Et dihedral angles (labeled Y and Z), while the third angle varies as a linear function of the other two. The surface maps the plane along the shortest paths between  $I_1$ ,  $I_2$ , and  $I_3$ , capturing the stark difference in the energy landscape and barrier heights between  $I_3$  and ( $I_1$ ,  $I_2$ ) compared to that between  $I_1$  and  $I_2$ . The color represents the energy in eV.

note that this assignment reveals that substantially all molecules are present in their lowest energy conformeric structure in the molecular beam, indicating that the conformational degrees of freedom are well cooled in the free jet expansion of TEA with the helium carrier gas.

While this assignment may appear tenuous, it is, in fact, the only choice that reconciles with the ensuing dynamics. Given the calculated minimum energy of  $I_3$  on the ion surface and its binding energy of 2.67 eV, we infer that the conformer  $R_3$  in the Rydberg state has an energy of 141 meV above the global minimum of the Rydberg conformer surface (see Figure 1).  $R_1$  and  $R_2$ , with binding energies between 2.7 and 2.87 eV, cannot be spectrally separated, and their energies in the Rydberg state are quite similar. The large energy difference of the  $R_3$  structure with respect to the ( $R_1$ ,  $R_2$ ) structure explains the rapid decay of the  $R_3$  signal observed in the time-resolved spectrum.

The excitation with 209 nm, followed by electronic relaxation from 3p to 3s, deposits a combined 1.2 eV of energy into vibrational coordinates. Given the set of vibrational frequencies calculated for the ion-state structure  $I_1$ ,<sup>27</sup> which we assume to closely approximate those in the 3s Rydberg state, and an adiabatic ionization potential of 7.47 eV,<sup>28</sup> we infer that the molecules are at equivalent temperatures of 760 K assuming equipartitioning of the energy. At that temperature we calculate that the equilibrium distributions of the conformers  $R_3$ ,  $R_2$ , and  $R_1$  should be 5%, 25%, and 70%, respectively. Indeed, in our time-dependent spectra we observe that the signal of the  $R_3$  conformer becomes very small, while that of the combined ( $R_1$ ,  $R_2$ ) conformer attains most of the intensity. The fit to the 3s peak (Figure 3a) shows that after 2 ps, 7% of the total signal remains in the  $R_3$  conformer while the rest (93%) is in  $R_1$ ,  $R_2$  conformations. This is in excellent agreement with the computational result.

In summary, from the experiment and the computation we find that most of the molecules are generated in the Rydberg state as the  $R_3$  conformer, but that this conformer decays to less than 7% of the total. The  $R_2$  and  $R_1$  conformers start with a negligible population, but their number grows to become the dominant (>93%) conformer. The near quantitative agreement between the computational and experimental results provides strong support for our assignment.

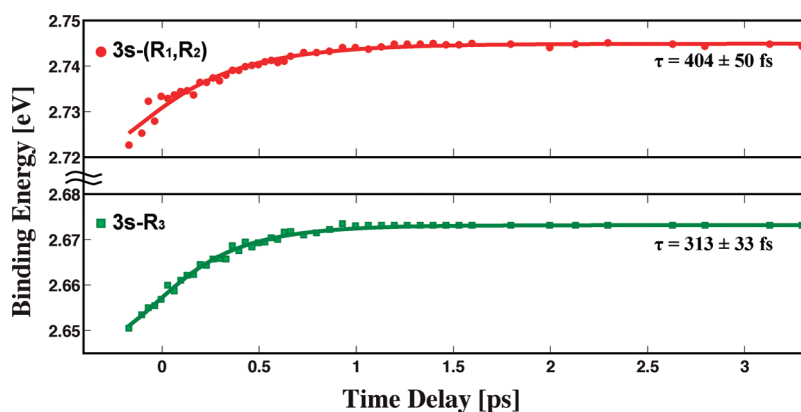


**Figure 5.** Peak position of  $3s\text{-}R_3$  and  $3s\text{-(}R_1,R_2\text{)}$  with respect to time. The time dependent peak positions were fitted assuming an exponential rise convoluted with the instrument function. The fitted time constants ( $\tau$ ) and  $3\sigma$  are  $313 \pm 33$  fs for  $3s\text{-}R_3$  and  $404 \pm 50$  fs for  $3s\text{-(}R_1,R_2\text{)}$ .

**Refinement of the Conformational Dynamics.** The broad peak in the range 2.7–2.87 eV, belonging to both conformers  $R_1$  and  $R_2$ , rises as the signal from conformer  $R_3$  decays. This peak is broadened beyond the experimental resolution, pointing to a dispersion of conformers with structures near the  $R_1$  and  $R_2$  energy minima. The structures  $R_1$  and  $R_2$  are quite similar, differing only in the rotation of a single ethyl group. The other ethyl groups do not hinder this rotation, so that transitions between the forms are facile. From the calculated ion energies and the range of the Rydberg binding energies we know that the  $R_1$  and  $R_2$  structures are part of a broad valley (Figure 4) in which different conformational forms coexist, at least at the high internal energy of TEA in this experiment.

A detailed analysis of the shape of the spectrum reveals that both the 2.67 and the 2.7–2.87 eV peak centers are moving toward higher energies on a time scale of several hundred femtoseconds, Figure 5. Apparently, as the molecules are generated in their respective energy valleys ( $R_3$  by excitation to the newly formed planar amine structure, ( $R_1,R_2$ ) from the decay of the  $R_3$  structure), they initially assume nonequilibrium conformational distributions with a dispersion about their minimum energy structures that leads to spectral peaks that are not centered with respect to the minimum. As the ethyl chains wiggle in the potential defined by their neighbors, the molecules approach their minimum energy structural distribution with time constants of  $313 \pm 33$  and  $404 \pm 50$  fs, respectively, for  $R_3$  and ( $R_1,R_2$ ), even while retaining the breadth of dispersion of conformational structures. We are watching, in real time, the process of the concerted and coupled ethyl motions settling into a shape that is determined by their mutual interactions.

## CONCLUSION AND PERSPECTIVES

By observing the time evolution of the Rydberg electron binding energy, we watch, in real time, how the dangling arms of the TEA molecule transition from their initial geometry to new conformational structures. Once there, the molecules jostle in the potential defined by the other parts of the molecule, approaching new equilibrium structures on a time scale of several hundreds of femtoseconds. Even so, the molecules retain a large amount of energy that enables them to assume a dispersion of structures about the minimum energy positions.

The experiment reveals in unprecedented clarity the kinetic and dynamic transformations between different conformational forms. In TEA, the dynamics on the Rydberg surface proceeds

in parallel to the electronic energy conversion between the Rydberg levels.

We note that for the close-lying minima in the energy landscape, the Rydberg electron binding energy is, even though varying slowly with the molecular shape, the determining parameter of the landscape. It stands to reason that the conformational energy landscape could be altered by exciting the molecules to different Rydberg states. With a wide range of angular momentum states accessible to one-photon or multiphoton excitation, it appears possible that the rate and outcome of conformational reactions can be tuned. Building on a large body of work to control the outcome of chemical reactions by suitable coherent or sequential radiation, this discovery opens the opportunity to optically control the conformational shape of floppy molecules.

## AUTHOR INFORMATION

### Corresponding Author

\*E-mail peter\_weber@brown.edu. Fax: +1-401-863-2594.

### Present Addresses

<sup>†</sup>Department of Chemistry, University of Chicago, Chicago, IL 60637.

## ACKNOWLEDGMENT

This project is supported by the Division of Chemical Sciences, Geosciences, and Biosciences, the Office of Basic Energy Sciences, the U.S. Department of Energy by grant number DE-FG02-03ER15452.

## REFERENCES

- (1) Munoz, V. Conformational dynamics and ensembles in protein folding. *Annu. Rev. Biophys. Biomol. Struct.* **2007**, *36*, 395–412.
- (2) Royer, C. A. Probing protein folding and conformational transitions with fluorescence. *Chem. Rev.* **2006**, *106*, 1769–1784.
- (3) Eklund, H.; Uhlin, U.; Farnegardh, M.; Logan, D. T.; Nordlund, P. Structure and function of the radical enzyme ribonucleotide reductase. *Prog. Biophys. Mol. Biol.* **2001**, *77*, 177–268.
- (4) Balzani, V.; Credi, A.; Silvi, S.; Venturi, M. Artificial nanomachines based on interlocked molecular species: recent advances. *Chem. Soc. Rev.* **2006**, *35*, 1135–1149.
- (5) Takeuchi, H.; Kojima, T.; Egawa, T.; Konaka, S. Molecular structures and conformations of Diethylamine and Triethylamine As Determined by Gas Electron Diffraction, ab Initio calculations, and vibrational spectroscopy. *J. Phys. Chem.* **1992**, *96*, 4389–4396.

- (6) Kuthirummal, N.; Weber, P. M. Rydberg states: sensitive probes of molecular structure. *Chem. Phys. Lett.* **2003**, *378*, 647–653.
- (7) Gosselin, J. L.; Weber, P. M. Rydberg fingerprint Spectroscopy: A new spectroscopic tool with local and global structural sensitivity. *J. Phys. Chem. A* **2005**, *109*, 4899–4904.
- (8) Kuthirummal, N.; Weber, P. M. Structure sensitive photoionization via Rydberg levels. *J. Mol. Struct.* **2006**, *787*, 163–166.
- (9) Stolow, A.; Bragg, A. E.; Neumark, D. M. Femtosecond time-resolved photoelectron spectroscopy. *Chem. Rev.* **2004**, *104*, 1719–1757.
- (10) Gessner, O.; et al. Femtosecond multidimensional imaging of a molecular dissociation. *Science* **2006**, *311*, 219–222.
- (11) Cheng, W.; et al. Control of Local Ionization and Charge Transfer in the Bifunctional Molecule 2-Phenylethyl-N,N-dimethylamine Using Rydberg Fingerprint Spectroscopy. *J. Phys. Chem. A* **2005**, *109*, 1920–1925.
- (12) Minitti, M. P.; Cardoza, J. D.; Weber, P. M. Rydberg Fingerprint Spectroscopy of Hot Molecules: Structural Dispersion in Flexible Hydrocarbons. *J. Phys. Chem. A* **2006**, *110*, 10212–10218.
- (13) Minitti, M. P.; Weber, P. M. Time-Resolved Conformational Dynamics in Hydrocarbon Chains. *Phys. Rev. Lett.* **2007**, *98*, 253004/1–253004/4.
- (14) Cheng, W.; Evans, C. L.; Kuthirummal, N.; Weber, P. M. A 9 eV superexcited state of 1,3-cyclohexadiene revealed by double resonance ionization photoelectron spectroscopy. *Chem. Phys. Lett.* **2001**, *349*, 405–410.
- (15) Rudakov, F. M.; Weber, P. M. Ground state recovery and molecular structure upon ultrafast transition through conical intersections in cyclic dienes. *Chem. Phys. Lett.* **2009**, *470*, 187–190.
- (16) Cardoza, J. D.; Weber, P. M. Resolved: Electronic states underneath broad absorptions. *J. Chem. Phys.* **2007**, *127*, 036101/1–036101/2.
- (17) Cardoza, J. D.; Rudakov, F. M.; Weber, P. M. Electronic Spectroscopy and Ultrafast Energy Relaxation Pathways in the Lowest Rydberg States of Trimethylamine. *J. Phys. Chem. A* **2008**, *112*, 10736–10743.
- (18) Gosselin, J.; Minitti, M. P.; Rudakov, F. M.; Solling, T. I.; Weber, P. M. Energy Flow and Fragmentation Dynamics of N, N-Dimethyl-isopropyl amine. *J. Phys. Chem. A* **2006**, *110*, 4251–4255.
- (19) Kawasaki, M.; Kasatani, K.; Hiroyasu, S.; Achiba, Y.; Sato, K.; Kimura, K. Multiphoton ionization of triethylamine: Determination of the vibrationless S<sub>2</sub> level by laser photoelectron spectroscopy. *Chem. Phys. Lett.* **1985**, *114*, 473–476.
- (20) Tannenbaum, E.; Coffin, E. M.; Harrison, A. J. The Far Ultraviolet Absorption Spectra of Simple Alkyl Amines. *J. Chem. Phys.* **1953**, *21*, 311–318.
- (21) Durig, J. R.; Craven, S. M.; Bragin, J. Low-Frequency Modes in Molecular Crystals. IX. Methyl Torsions and Barriers to Internal Rotation of Some Three-Top Molecules. *J. Chem. Phys.* **1970**, *53*, 38–50.
- (22) Kim, B.; Thant, N.; Weber, P. M. High-resolution photoelectron spectroscopy: the vibrational spectrum of the 2-aminopyridine cation. *J. Chem. Phys.* **1992**, *97*, 5384–5391.
- (23) Cureton, C. G.; Hara, K.; O'Connor, D. V.; Phillips, D. The photophysics of tertiary aliphatic amines. *Chem. Phys.* **1981**, *63*, 31–49.
- (24) Rianda, R.; Frueholz, R. P.; Goddard, W. A. The low lying states of ammonia; generalized valence bond and configuration interaction studies. *Chem. Phys.* **1977**, *19*, 131–136.
- (25) The oscillator strengths of the optical transitions to 3p states were calculated using standard computational packages. The analysis is the same as the one applied earlier to Trimethylamine (see ref 1717).
- (26) Frisch, M. J.; Trucks, G. W.; Schlegel, H. B.; Scuseria, G. E.; Robb, M. A.; Cheeseman, J. R.; Montgomery, Jr., J. A.; Vreven, T.; Kudin, K. N.; Burant, J. C.; Millam, J. M.; Iyengar, S. S.; Tomasi, J.; Barone, V.; Mennucci, B.; Cossi, M.; Scalmani, G.; Rega, N.; Petersson, G. A.; Nakatsuji, H.; Hada, M.; Ehara, M.; Toyota, K.; Fukuda, R.; Hasegawa, J.; Ishida, M.; Nakajima, T.; Honda, Y.; Kitao, O.; Nakai, H.; Klene, M.; Li, X.; Knox, J. E.; Hratchian, H. P.; Cross, J. B.; Bakken, V.; Adamo, C.; Jaramillo, J.; Gomperts, R.; Stratmann, R. E.; Yazyev, O.; Austin, A. J.; Cammi, R.; Pomelli, C.; Ochterski, J. W.; Ayala, P. Y.; Morokuma, K.; Voth, G. A.; Salvador, P.; Dannenberg, J. J.; Zakrzewski, V. G.; Dapprich, S.; Daniels, A. D.; Strain, M. C.; Farkas, O.; Malick, D. K.; Rabuck, A. D.; Raghavachari, K.; Foresman, J. B.; Ortiz, J. V.; Cui, Q.; Baboul, A. G.; Clifford, S.; Cioslowski, J.; Stefanov, B. B.; Liu, G.; Liashenko, A.; Piskorz, P.; Komaromi, I.; Martin, R. L.; Fox, D. J.; Keith, T.; Al-Laham, M. A.; Peng, C. Y.; Nanayakkara, A.; Challacombe, M.; Gill, P. M. W.; Johnson, B.; Chen, W.; Wong, M. W.; Gonzalez, C.; and Pople, J. A. *Gaussian 03*, Revision C.02, Gaussian, Inc.: Wallingford, CT, 2004.
- (27) The normal-mode frequencies obtained in our DFT calculation are, in cm<sup>-1</sup>, 54, 94, 104, 163, 210, 240, 270, 293, 298, 412, 446, 584, 706, 811\*, 919\*, 953, 989\*, 1054, 1069, 1102, 1120, 1213\*, 1281, 1332, 1341, 1392\*, 1415\*, 1424, 1479\*, 1494\*, 1509\*, 3023\*, 3053\*, 3121\*, 3133\*, 3143\*; the asterisks indicate degenerate vibrations.
- (28) Mathis, J. E.; Compton, R. N. Single and multiple photon ionization of triethylamine. *J. Chem. Phys.* **1996**, *104*, 8341–8347.